N O T I C E

THIS DOCUMENT HAS BEEN REPRODUCED FROM MICROFICHE. ALTHOUGH IT IS RECOGNIZED THAT CERTAIN PORTIONS ARE ILLEGIBLE, IT IS BEING RELEASED IN THE INTEREST OF MAKING AVAILABLE AS MUCH INFORMATION AS POSSIBLE

DOE/NASA/51040-21
NASA TM-81648

A Four-Cylinder Stirling Engine Controls Model

Carl F. Lorenzo and Carl J. Daniele
National Aeronautics and Space Administration
Lewis Research Center

Work performed for
U.S. DEPARTMENT OF ENERGY
Conservation and Solar Energy
Office of Transportation Programs

Prepared for
1980 Automotive Technology Development
Contractor Coordination Meeting
Dearborn, Michigan, November 11-13, 1980

DOE/NASA/51040-21
NASA TM-81648

A Four-Cylinder Stirling Engine Controls Model

Carl F. Lorenzo and Carl J. Daniele
National Aeronautics and Space Administration
Lewis Research Center
Cleveland, Ohio 44135

Work performed for
U.S. DEPARTMENT OF ENERGY
Conservation and Solar Energy
Office of Transportation Programs
Washington, D.C. 20545
Under Interagency Agreement DE-AI01-77CS51040

Prepared for
1980 Autcmotive Technology Development
Contractor Coordination Meeting
Dearborn, Michigan, November 11-13, 1980

A FOUR-CYLINDER STIRLING ENGINE CONTROLS MODEL*

by Carl F. Lorenzo and Carl J. Daniele

NASA Lewis Research Center
Cleveland, Ohio 44135

SUMMARY

A four working space, double-acting piston, Stirling engine simulation is being developed for controls studies. The development method is to construct two simulations, one for detailed fluid behavior, and a second model with simple fluid behaviour but containing the four working space aspects and engine inertias, validate these models separately, then upgrade the four working space model by incorporating the detailed fluid behaviour model for all four working spaces.

The single working space (SWS) model contains the detailed fluid dynamics. It has seven control volumes in which continuity, energy, and pressure loss effects are simulated. Comparison of the SWS model with experimental data shows reasonable agreement in net power versus speed characteristics for various mean pressure levels in the working space.

The four working space (FWS) model was built to observe the behaviour of the whole engine. The drive dynamics and vehicle inertia effects are simulated. To reduce calculation time, only three volumes are used in each working space and the gas temperatures are fixed (no energy equation). Comparison of the FWS model predicted power with experimental data shows reasonable agreement. Since all four working spaces are simulated, the unique capabilities of the model are exercised to look at working fluid supply transients, short circuit transients, and piston ring leakage effects. The FWS model has been upgraded by using the detailed SWS model for each of the four working spaces. Currently the detailed FWS model is being reworked to reduce the amount of calculation time per cycle.

NOMENCLATURE

A	area, m^2
c_p	specific heat at constant pressure, J/(kg-K)
c_v	specific heat at constant volume, J/(kg-K)
F	force, N
f( )	function of
G	gear ratio
h	heat transfer coefficient, J/(sec-m^2-K)
I	inertia, N-m-sec^2
J	mechanical equivalent of heat, 1.0 (N-m)/J

*Work performed for the U.S. Department of Energy under Interagency Agreement DE-AI01-77CS51040.

k	resistance, (N-sec)/kg
ℓ	piston stroke, m
P	pressure, N/m^2
Q	heat flow rate, J/sec
R	gas constant, (N-m)/(kg-K)
R_l	connecting rod length, m
$\mathscr{R}$	fluid resistance, $(N\text{-sec})/(kg\text{-}m^2)$
T	temperature, K
t	time, sec
$\mathscr{T}$	torque, N-m
V	volume, m
Vel	vehicle velocity, km/hr
W	mass, kg
w	mass flow rate, kg/sec
γ	ratio of specific heats
Δ	change in
θ	angular position, rad

Subscripts:

a	auxiliaries
c	cooler
d	drag
e	engine
f	mechanical friction
h	heater wall
i	position in working space, index
in	into
j,k	working space
ℓ	piston ring leakage
m	mesh
o	dead volume
out	out of
p	piston
r	rod
rl	rod leakage
rr	rolling resistance
s	stored
SHT	short circuit
SHTMAX	short circuit maximum
SHTMIN	short circuit minimum
sup	supply
volume	gas volume
w	wheel

INTRODUCTION

A four working space, double-acting piston, Stirling engine simulation is being developed at the NASA Lewis Research Center for controls studies (ref. 1). The development method is to construct two simulations which together form a complete model. The models are: a single working space model, with detailed fluid behaviour, and a second model, with simple fluid behaviour but containing the four working space aspects and the engine

mechanical inertias. The approach is to then combine them into a single detailed controls model. The single working space (SWS) model was developed to determine the number of control volumes (lumps) and equation types needed to adequately represent the thermodynamics of the engine. The SWS model has been written to approximate a detailed performance model (ref. 2) developed by Tew. The SWS model differs from the performance model in that the SWS model has fewer control volumes, includes integrated flow pressure drop effects and uses average values of heat transfer coefficients and flow resistances determined from the performance model results. Also the SWS model does not contain shuttle or conduction losses since these influence efficiency but do not impact control behaviour.

A second model was constructed to study the behaviour of the total engine system. The model consists of four working spaces (FWS) between four pistons. To reduce the calculation time on the digital computer, only three control volumes are used in each working space and gas temperatures are fixed within each volume (no energy equation). The drive dynamics are also included and the FWS model can be run either by forcing the piston motion or as an engine.

Included in this paper are results obtained from both models and comparisons with some experimental data. Also, since all four working spaces are simulated, the unique capability of the FWS model is exercised to study various phenomena not easily duplicated by a single working space model. To demonstrate this capability, working fluid supply transients, short circuit (braking) effects, and piston ring leakage performance are presented.

Finally, the capabilities of both models have been combined into a single detailed controls simulation which will eventually be used with a detailed engine control system simulation to explore various controls concepts.

SINGLE WORKING SPACE (SWS) MODEL

A single working space model of a Stirling engine was developed to determine an adequate representation for the fluid dynamics and thermodynamics of the engine. Seven control volumes were selectedone each for the expansion space and heater, three for the regenerator to give a reasonable temperature distribution, and one each for the cooler and compression spaces. A schematic of the model is shown in figure 1.

SWS Model Equations

The equations used to model the fluid dynamics and thermodynamics are simplifications to the complex partial differential flow equations. Mass flow is assumed to occur due to pressure differential between gas modes. From figure 1, some representative equations for mass flow are

$$\dot{w}_i = \frac{1}{\mathcal{R}_{i \to i+1}} \left(P_i - P_{i+1} \right) \qquad i = 1,2, \ldots 6 \tag{1}$$

The change in stored mass in a volume is:

$$\dot{w}_{s_i} = \dot{w}_{i-1} - \dot{w}_i \qquad \begin{matrix} i = 1,2, \ldots 7 \\ \dot{w}_0 = \dot{w}_7 = 0.0 \end{matrix} \tag{2}$$

The energy equation used to calculate the change in temperature in a volume is complex due to the oscillatory nature of the Stirling cycle. The form of the equation (ref. 3) is;

$$w_{s_i} T_i = \dot{w}_{i-1}\left(\gamma T'_{i-1} - T_i\right) - w_i\left(\gamma T'_i - T_i\right) + \frac{\Sigma \dot{Q}}{c_v} + \frac{\Sigma \text{Work}}{J c_v} \qquad \begin{matrix} i = 1,2, \ldots 7 \\ \dot{w}_0 = \dot{w}_7 = 0.0 \end{matrix} \tag{3}$$

where the heat flows to and from the gas are modeled as:

$$\dot{Q} = hA(\Delta T) \tag{4}$$

The primed variables are interface volume temperatures and are determined by upwind differencing (ref. 2). The method assumes that the gas temperatures have the same temperature profile as the regenerator matrix temperature. A representative equation is:

$$\left.\begin{aligned} &\dot{w}_i \geq 0 \quad T'_i = T_i - \frac{\left(T_{m_3} - T_{m_5}\right)}{4.0} + \frac{\dot{w}_i \Delta t \left(T_{m_3} - T_{m_5}\right)}{4.0\, w_{s_i}} \\ &\dot{w}_i < 0 \quad T'_i = T_{i+1} - \frac{\left(T_{m_3} - T_{m_5}\right)}{4.0} + \frac{\dot{w}_i \Delta t \left(T_{m_3} - T_{m_5}\right)}{4.0\, w_{s_{i+1}}} \end{aligned}\right\} 2 \leq i \leq 5$$

$$\left.\begin{aligned} &\dot{w}_i \geq 0 \quad T'_i = T_i \\ &\dot{w}_i < 0 \quad T'_i \quad T_{i+1} \end{aligned}\right\} i = 1,6 \tag{5}$$

The regenerators are modeled as thermal lags:

$$\dot{T}_{m_i} = \frac{h_i A_i}{c_{p_m} w_{s_m}} \left(T_i - T_{m_i}\right) \qquad i = 3,4,5 \tag{6}$$

Pressure is calculated using the ideal gas law based on volume temperatures. Variable volumes are calculated using the drive geometry to calculate piston position as a function of crank angle. These equations are described later.

Equations of the forms of (2), (3), and (6) for the seven volumes result in a 17th order model. The integration technique used is a backward difference method which utilizes a multivariable Newton-Raphson iteration (ref. 4). This technique was chosen because of the large difference in time constants which results when flow resistance is considered.

Comparison of the SWS model with the Tew performance model shows agreement of pressures within 2 percent and temperatures within 8 percent over a cycle at steady state. This is considered adequate for controls analysis where performance detail is not so important.

FOUR WORKING SPACE (FWS) MODEL

The second model generated was a four working space model. Since the purpose of the model was to investigate the four working space aspects of the whole engine, the fluid dynamic model of each working space was simplified. Only three control volumes are used in each working space. One volume for the heater (and expansion) space, one volume for the regenerator, and one volume for the cooler (and compression) space. All volumes are assumed isothermal-with the expansion and compression space gas temperatures being the average steady state temperatures from the SWS model. The regenerator gas and mesh temperatures are assumed to be the same. While the model is quite simple it will be shown that it gives a fairly good representation of the engine. The model also has the drive dynamics included as well as a simple model for vehicle load effects. A schematic of the model is shown in figure 2.

FWS Model Equations

The fluid dynamic equations used in the FWS model are simplified from the SWS model. From figure 2, the pistons are numbered in the order in which they reach top stroke as is indicated by the arrows in the piston heads. Double subscripted variables indicate; first subscript, a volume position within a working space; second subscript, the working space. Some representative equations are:

$$\left.\begin{aligned} \dot{w}_{i,j} &= \left(P_{i,j} - P_{i+1,j}\right) \Big/ R_{i,j \to i+1,j} && j = 1,4 \\ & && i = 1,2 \\ \dot{w}_{s_{i+1,j}} &= \dot{w}_{i,j} - \dot{w}_{i+1,j} && j = 1,4 \\ & && i = 1,3 \\ & && \dot{w}_{0,j} = \dot{w}_{3,j} = 0.0 \end{aligned}\right\} \quad (8)$$

and

$$P_{i,j} = w_{s_{i,j}} RT_{i,j} \Big/ V_{i,j} \qquad \begin{aligned} j &= 1,4 \\ i &= 1,3 \end{aligned} \quad (9)$$

Variable volumes are calculated as a function of piston position:

$$V_{1,1} = V_{1,1_0} + \left(\frac{\ell}{2} - X_1\right) A_p \quad (10)$$

Piston position is a function of crank angle:

$$X_i = \left(\frac{\ell}{2}\right) \cos \theta_i + \sqrt{R_L^2 - \left(\frac{\ell}{2}\right)^2 \sin^2 \theta_i} - \sqrt{R_L^2 - \left(\frac{\ell}{2}\right)^2} \qquad i = 1,2 \ldots 4 \quad (11)$$

Torque is calculated as a function of differential forces on the pistons which are summed through the drive geometry:

$$T_1 = \left(\frac{\ell}{2}\right)\left[P_{1,1}A_p - P_{3,2}\left(A_p - A_r\right)\sin\theta_1\right]\left(1 + \frac{\left(\frac{\ell}{2}\right)\cos\theta_1}{\sqrt{R_L^2 - \left(\frac{\ell}{2}\right)^2\sin^2\theta_1}}\right) \quad (12)$$

Also included in the FWS model are simplified vehicle load effects and engine power losses due to mechanical friction and auxiliaries. Figure 3 shows a schematic of how these losses are calculated. Torques from the four pistons are summed to form indicated torque. Torque due to engine friction ($\mathcal{T}_f$) is subtracted to form brake torque. This is then available for auxiliaries ($\mathcal{T}_a$) and also for vehicle load effects such as rolling resistance ($\mathcal{T}_{rr}$) and drag ($\mathcal{T}_d$). The vehicle inertia is brought into the torque equation through the gear ratio to give an effective engine inertia. The summation of torques is integrated to give engine speed and integrated again to give crank angle, θ_i, which in turn is used to generate piston position (eq. (11)). The torque equations for the losses are linear and nonlinear functions of θ with the torque equation:

$$I_{eff}\ddot{\theta}_e = \mathcal{T}_1 + \mathcal{T}_2 + \mathcal{T}_3 + \mathcal{T}_4 - \mathcal{T}_f(\dot{\theta}) - \mathcal{T}_a(\dot{\theta}) - \mathcal{T}_d(\dot{\theta}) - \mathcal{T}_{rr}(\dot{\theta}) \quad (13)$$

COMPARISON OF FWS AND SWS MODELS WITH EXPERIMENTAL DATA

Both the SWS and FWS models were run at various engine speeds from 1000 to 4000 rpm and three different mean pressure levels ranging from 5 to 15 MPa. Power was calculated for each cycle until steady state was reached. Power calculations were made by integrating the area of the pressure-volume curves in the expansion and compression spaces; and then adding the results at the end of the cycle. The power output predicted by the SWS model was multiplied by four to give gross engine power. The FWS model sums up the predicted power (indicated) from all four working spaces. From these values, mechanical and auxiliary power losses are subtracted to get net power. The results are shown in figure 4. Both models show reasonable agreement over the whole map with the SWS model showing slightly better agreement than the FWS model at the higher mean pressures and speeds, although neither model predicted the fall in power at 4000 rpm and 15 MPa.

UNIQUE CAPABILITIES OF THE FWS MODEL

The purpose of the models discussed in this report is for controls studies. The FWS model is simplified but can be used to study overall engine performance in response to various control schemes and inputs. Also since all four working spaces are simulated, the FWS model can be used to study phenomena not easily duplicated by a single working space model. Some applications of these will now be shown.

Working Fluid Supply Transient

The mean pressure control system for Stirling engines modulates engine power by changing the amount of working fluid in the cycle. In order to increase engine speed, working fluid is supplied to the engine. A slot in the piston rod is used to time the injection of working fluid into the various compression spaces of the engine (fig. 5). The timing is arranged to supply the fluid only when the pistons are near bottom (min) stroke. During this period, the pressure in the space is near maximum and the injected fluid functions to increase rather than decrease (temporarily) the engine torque. The check values (fig. 5) remain open as long as the supply pressure is greater than the corresponding compression space pressure. The supply flow through the timing slot is modeled as (no leakage case):

$$\dot{w}_{sup_i} = \begin{cases} \dfrac{A_{sup_i}(x_i)}{k_i}\left(P_{sup} - P_{3,i}\right) & i = 1, \ldots, 4 \\ & P_{sup} \geq P_{3,i} \\ 0 & P_{sup} < P_{3,i} \end{cases} \qquad (14)$$

where $A_{sup_i}(x_i)$ is the timing slot area as a function of stroke as indicated in the block diagram (fig. 6). When leakage around the piston rod is considered, an additional flow in parallel with w_{sup_i} is modeled:

$$\dot{w}_{r\ell_i} = \begin{cases} \dfrac{A_{r\ell_i}}{k_{r\ell_i}}\left(P_{sup_i} - P_{3,i}\right) & i = 1, \ldots, 4 \\ & P_{sup} \geq P_{3,i} \\ 0 & P_{sup} < P_{3,i} \end{cases} \qquad (15)$$

In this equation $A_{r\ell_i}$ is the effective leakage area around the piston rod, not including the timing slot area. The area $A_{r\ell_i}$ will normally be considered as a percentage of the maximum slot area A_i. A typical supply transient is shown in figure 7. The initial engine speed is 2000 rpm. After the simulation settles out, working fluid is added. This is shown as a function of time in the top graph. Note that the amount of working fluid added decreases with each cycle since the working space pressure level continues to rise. Only the supply for the second working space is shown. Supplies for the other working spaces are similar but phase shifted by 90° with some overlap. Note the increase in torque amplitude when injection begins. This is due to the timing effect of the injections. Also, as fluid is added, the compression space pressure rises.

The torque wave shape shows four cycles (4x) for every engine cycle before the supply transient starts. This is due to the summation of torque from all four pistons. During the fluid supply process, the fundamental en-

gine frequency is dominant. However, the 4x frequency is still seen in the torque transient.

When the working fluid is added to the cycle, the torque starts to rise and a corresponding speed increase is seen. There is no transient torque drop seen in these results. This is probably due to the absence of the energy equation for the incoming fluid in the compression space. The addition of cold working fluid to the compression space in the actual engine has a quenching effect on the temperature causing pressure to drop which results in a taransient drop in torque. Other factors that might also cause a transient torque drop, include piston rod leakage and the crank angle at which injection begins.

An understanding of the torque wave shape may be obtained by considering all the injected flows and the effects on pressures and individual torques generated by each piston. These variables are plotted together in figure 8. Since the pressure differences in any given working space are small at a given time, only the compression space pressure is plotted. The supply pressure is increased to 13.8 MPa at $t = 0.06$ second. Initially working fluid is injected into working space number 3 (see fig. 2). This has the effect of increasing the pressure P_{comp_3}. The effect on peak pressure in this space, however, is not seen until the next time. P_{comp_3} reaches its peak pressure, at approximately $t = 0.09$ second. Compression spaces 4, 1, and 2, respectively, receive injections of working fluid as time progresses and the process continues until the working space pressures increase to a level at which fluid can no longer be supplied (eq. (14)). The effect of the increased pressure (P_{comp_3}) in working space number 3 is to increase the torque output of piston number 3 and decrease the torque output of piston number 2. However, in the interpretation of the individual torques generated by the various pistons, it should be noted that each piston sees both a positive and negative acting pressure since the pistons are double acting. For example, in this transient the net effect of P_{comp_3} and P_{comp_4} is to reduce somewhat the peak torque on piston number 3 occurring at approximately $t = 0.09$ second. This happens because working space number 3 received only about half the amount of working fluid received by working space number 4 during the first charge sequence. The addition of the individual torques then gives the total indicated torque. The indicated torque along with losses and auxiliary effects are integrated using the engine equation of motion (eq. (13)) to give the engine speed.

Piston Rod Leakage

The effect of working fluid leakage around the piston rod is shown in figure 9. For this study the leakage area A_{rl_i} is taken to be one half the maximum area of the piston rod slot A_i (refer to fig. 6). The leakage area is the same for all four piston rods. The leakage is indicated by the non-zero baseline flows observed in the plots of the individual flows $\dot{w}_{sup_i}$. Similar increases are seen in the levels of the individual compression space pressures and the individual torques. The total torque also increases and the 4x frequency is observed throughout the charging transient.

A comparison of the total indicated torques for three levels of piston rod leakage is shown in figure 10. The total torque for the case of $A_{r\ell_j} = 0.1\ A_j$ is substantially the same as the no-leakage case (fig. 8). When placed on the same scale, only a very small increase is seen. Expected leakage areas will probably not exceed $A_{r\ell_j} = 0.2\ A_j$. The higher levels are plotted for comparison purposes. It is noted that, as the leakage rate increases, the amplitude of the fundamental (engine frequency) component of total torque decreases.

A more interesting aspect of rod leakage is the case in which a single rod leaks (fig. 11). Again, the charging transient begins at $t = 0.06$ second. A leakage area $A_{r\ell_j} = 0.5\ A_j$ has been selected to exaggerate the effects which occur. The leaking rod gives an added injected flow into working space number 1. This is really observed in the supply flows. The effect is to increase the pressure in that space relative to the others. This increases the torque produced by piston number 1 but decreases that of piston number 4. This unbalance in torque generated by the individual pistons gives rise to high amplitude oscillations in total indicated torque during the charging transient. In a real engine piston ring leakage would reduce the amplitude of oscillation below that observed in this case.

The torque oscillations are also manifested in the speed response. The effects on the total indicated torque as the piston rod leakage increases is shown in figure 12. The engine frequency (fundamental) oscillations are seen to increase as leakage area increases. Also the effects of the 4x frequency component is reduced (relative to the fundamental) as the leakage rate increases. This is apparent when compared with figure 10, where the leakage of all piston rods is the same.

The transient torque reversal is not seen when piston rod leakage is included in the model. Two factors may be responsible for this: (1) the quenching effect mentioned in the previous section which is not yet treated in the model and (2) the simplified supply model. That is, in the assumed supply model feedline inductance and compliance have not been included; (i.e., no pressure node is simulated downstream of the check valve).

Piston Ring Leakage

The next effect studied is piston ring leakage. This allows working fluid to pass from one working space to an adjacent one. This analysis would be difficult to duplicate on a single working space model since the flow can redistribute through all four working spaces. It is assumed in this analysis that all four piston rings have the same leakage area. The leakage terms are designated as $\dot{w}_\ell$ in figure 2. The leakage flow is modeled using an orifice equation:

$$\dot{w}_{\ell_{j,k}} = 0.90\ A_\ell \sqrt{\frac{2g\left(P_{i,j} - P_{3,k}\right)}{R\left(T_{i,j} - T_{3,k}\right)}}\ \sqrt{P_{i,j} - P_{3,k}} \qquad \begin{array}{l} j = 1,2, \ldots 4 \\ k = j + 1 \\ \text{if } j = 4,\ k = 1 \end{array} \qquad (16)$$

The results are shown in figure 13. The nominal leakage area chosen was 0.002 cm^2 which corresponds to a gap of about 0.00025 cm. The resultant effective leakage flow resistance at 15 MPa mean pressure and 4000 rpm is about 30 times greater than the flow resistance in the working spaces. This results in a maximum flow rate 130 times larger in the working spaces than through the leakage area. The maximum flow rate ratio drops with speed to 30 at 1000 rpm and 15 MPa; and with leakage area increase, to 34 at 1000 rpm and 0.008-cm leakage area. The simulation was run at four different engine speeds from 1000 to 4000 rpm and six different leakage areas from 0 to 0.01 cm^2. The indicated power was recorded when steady state was reached and then the mechanical and auxiliary power losses were subtracted from it as was done in figure 4. Note that the A = 0 case is the same as plotted on figure 4. As the leakage flow area increased, the resultant net power of the engine dropped. For a leakage area of 0.004 cm^2, a power reduction of 12 percent at 4000 rpm and almost 34 percent at 1000 rpm was observed. This analysis shows the value of a four working space model to predict power losses that can occur due to faulty piston rings in a Stirling engine. The effects of a failure of a single ring can also be easily investigated with a four working space model of this type.

Short Circuit Analysis

Rapid engine braking of the Stirling engine is accomplished by short circuiting of the working spaces. The analysis of a short circuit control mode is most effectively done with a four working space engine model. Figure 14 shows a schematic of the short circuit system. The compression space of each working space is connected to two different plenums, one containing a high pressure (P_{SHTMAX}) and one containing a low pressure (P_{SHTMIM}). Check valves allow flow to the nigh pressure plenum when the corresponding compression space pressure is greater than P_{SHTMAX}. A second set of check valves let flow to the compression space when the corresponding compression space pressure is lower than P_{SHTMIN}. Thus working fluid is removed from the compression space when the pressure is at a maximum thereby lowering the maximum pressure; and added to the compression space when the pressure is at a minimum thereby increasing the minimum pressure. The system thus decreases the pressure swing in the working spaces and thus lowers the power output of the engine. A valve connects the two plenums and determines the amount of engine braking that is accomplished. With the valve shut, the plenum pressures reach their respective maximum and minimum values. With the valve open, pressure in the high pressure plenum falls and pressure in the low pressure plenum rises. Note that the system requires working fluid to be shuttled to and from two different plenums and four working spaces. This would very difficult to simulate using only a single working space model.

Figure 15 shows the net steady state power as a function of speed and valve opening ratio. Note the large drop in power as the valve is open for any constant speed. For example, if the valve is half open, the power drops from 34.5 to 1.25 kW at 4000 rpm. If the valve is open sufficiently, the power goes negative which indicates the engine is absorbing power from the load. The data for these curves was obtained by forcing piston position as a function of time (drive dynamics not active) and letting the simulation

settle out. At the highest valve openings (0.5 to 1.0) the power starts to increase as speed drops.

The torque curves corresponding to the power curves in figure 15 are shown in figure 10. Note that the torque also drops significantly with valve opening at constant speed. At 4000 rpm, it drops from 86 to 0 N-m at 0.5 area ratio. As speed decreases, torque continues to drop off for the higher valve area settings. Figures 15 and 16 indicate that short circuiting is a very effective means of supplying engine braking torque.

SUMMARY

Presented in this report are preliminary results from a simplified four working space Stirling engine simulation. The model was constructed to simulate overall engine behaviour, rather than precise performance, for controls studies. While the model is quite simple, it exhibits reasonable results when compared to steady-state engine test results, and gives both steady-state and transient results which are representative of Stirling engine behaviour. Also presented is a single working space model which has a detailed model of the fluid dynamic and thermodynamic aspects of a single working space. This model also shows reasonable results when compared to experimental data. Currently, the FWS model has been upgraded by incorporating the detailed fluid behaviour model for all four working spaces. This detailed model will be a reference model for Stirling engine controls studies. The simplified models will be normally used when they yield valid results. But, in some cases, such as short circuiting, a detailed four working space model is required. Results from the detailed model should compare even more favorably with the Stirling engine behaviour since the heat transfer characteristics of the different phenomena simulated can be incorporated into the model. For example, the quenching effect of the cold supply fluid on the compression space temperature can be included. This could result in a better prediction of the torque waveshape during a supply transient. Future efforts will include conceptual controls studies such as variable stroke control and detailed modeling of the current mean pressure control.

REFERENCES

1. Daniele, Carl J.; and Lorenzo, Carl F.: Preliminary Results From a Four-Working Space, Double Acting Piston, Stirling Engine Controls Model. DOE/NASA/1040-17, NASA TM-81569, 1980.

2. Tew, R. C.; Jefferies, K., and Miao, D., "A Stirling Engine Computer Model for Performance Calculations." DOE/NASA/1011-78/24, NASA TM-78884, 1978.

3. Daniele, C. J. and Lorenzo, C. F., "Dynamic Analysis of a Simplified Free-Piston Stirling Engine," Simulation, Vol. 34, No. 6, June 1980, pp. 195-206.

4. Sellers, J. F. and Daniele, C. J., "DYNGEN - A Program for Calculating Steady-State and Transient Performance of Turbojet and Turbofan Engines," NASA TN D-7901, 1975.

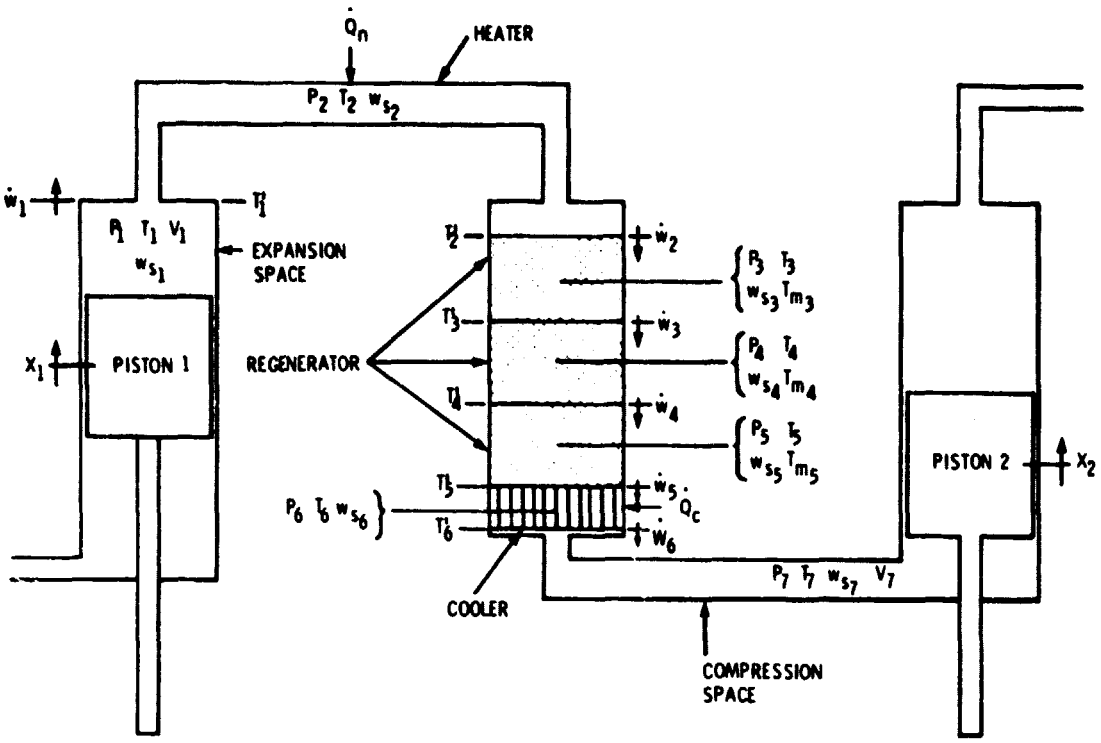

Figure 1. - Schematic of a single working space (SWS) model.

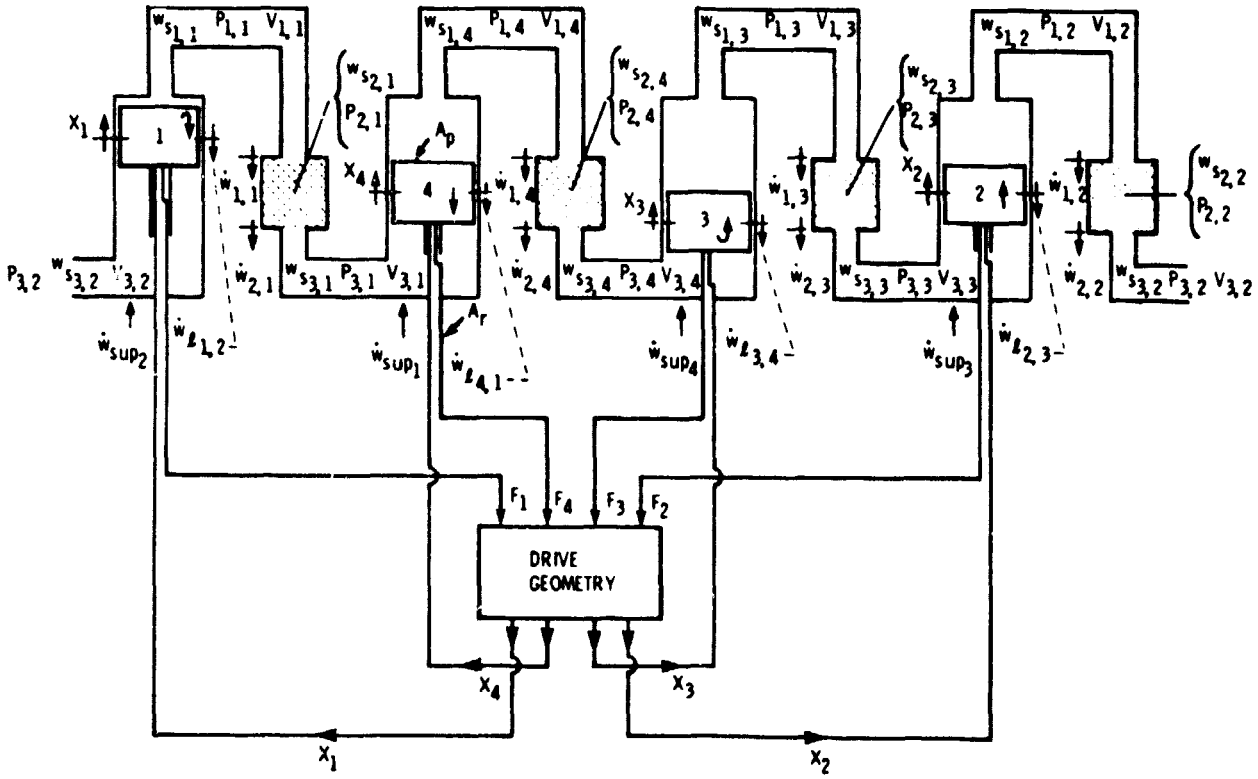

Figure 2. - Schematic of four working space (FWS) model.

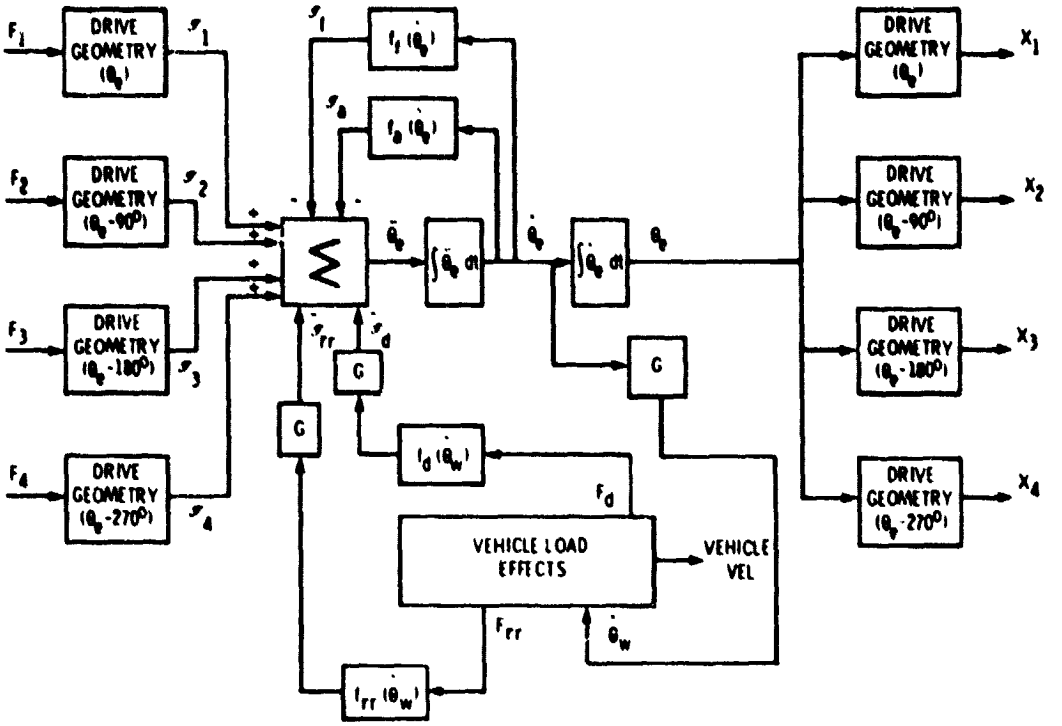

Figure 3 - Stirling engine drive dynamics.

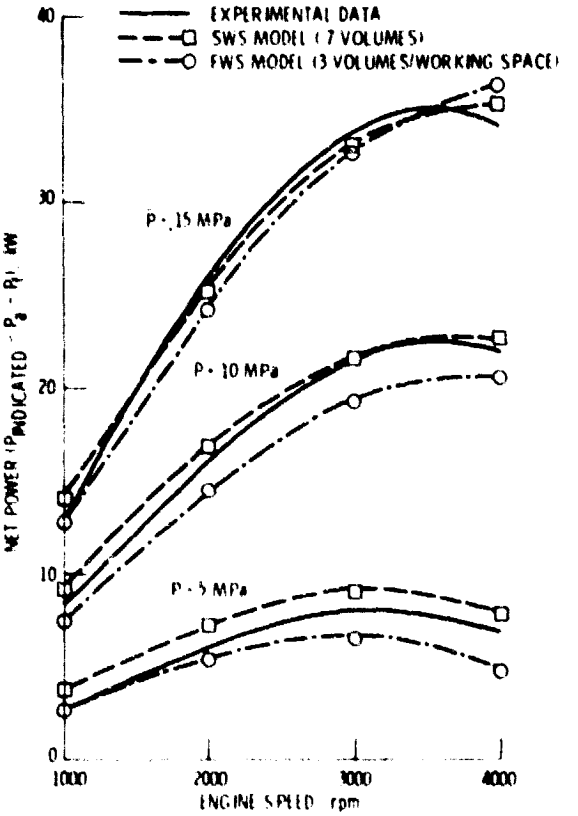

Figure 4 - Comparison of net power versus speed for the SWS and FWS models and engine data

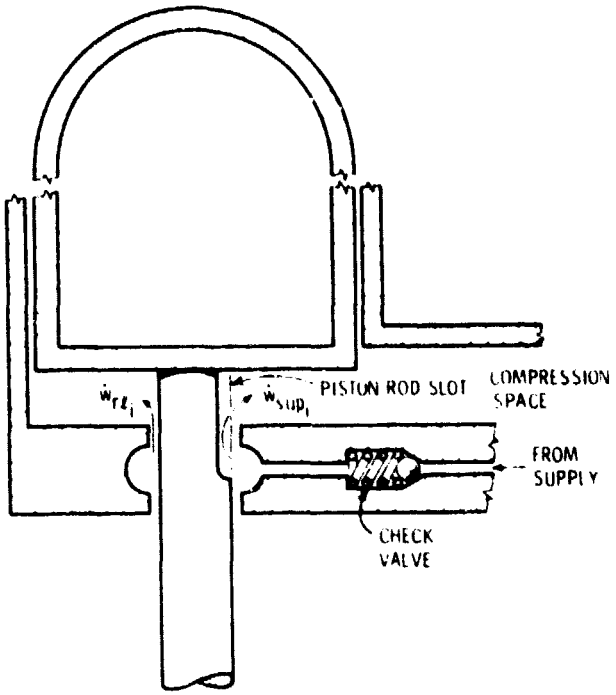

Figure 5. Working fluid supply system.

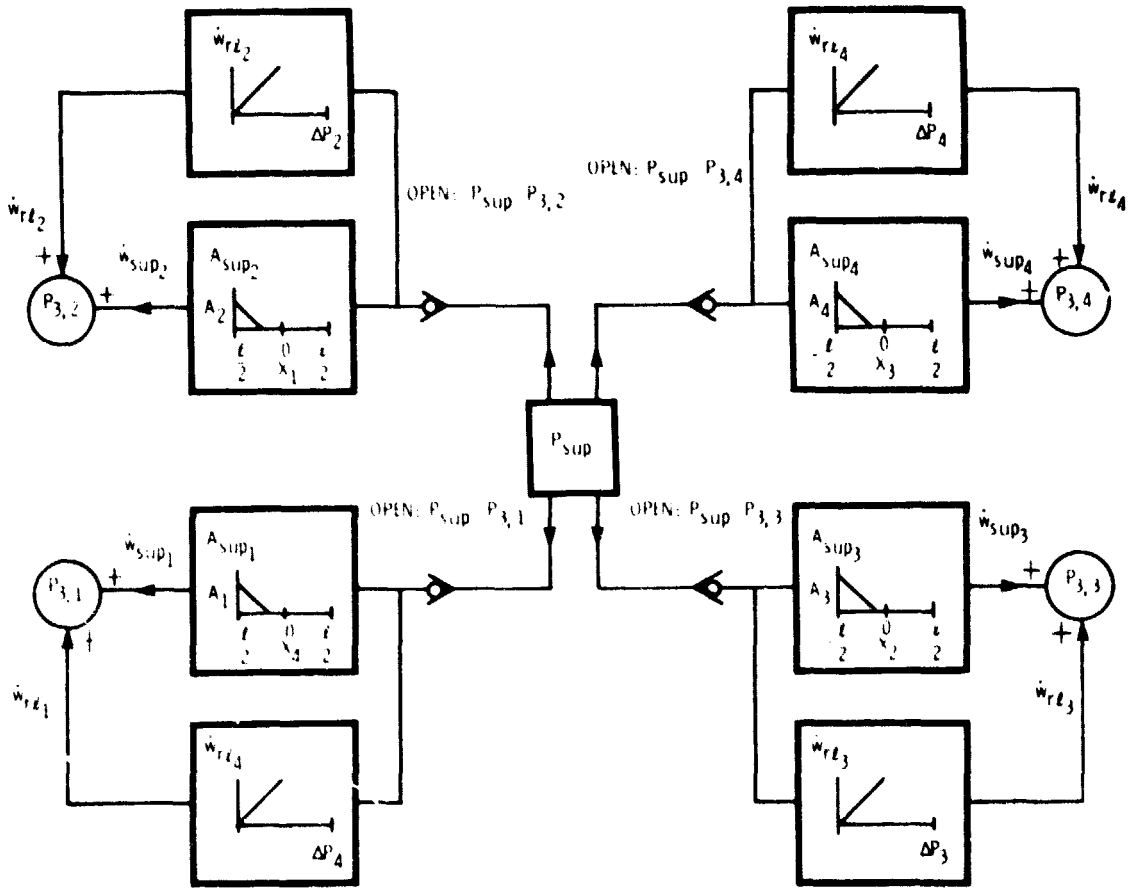

Figure 6. Schematic of working fluid supply system.

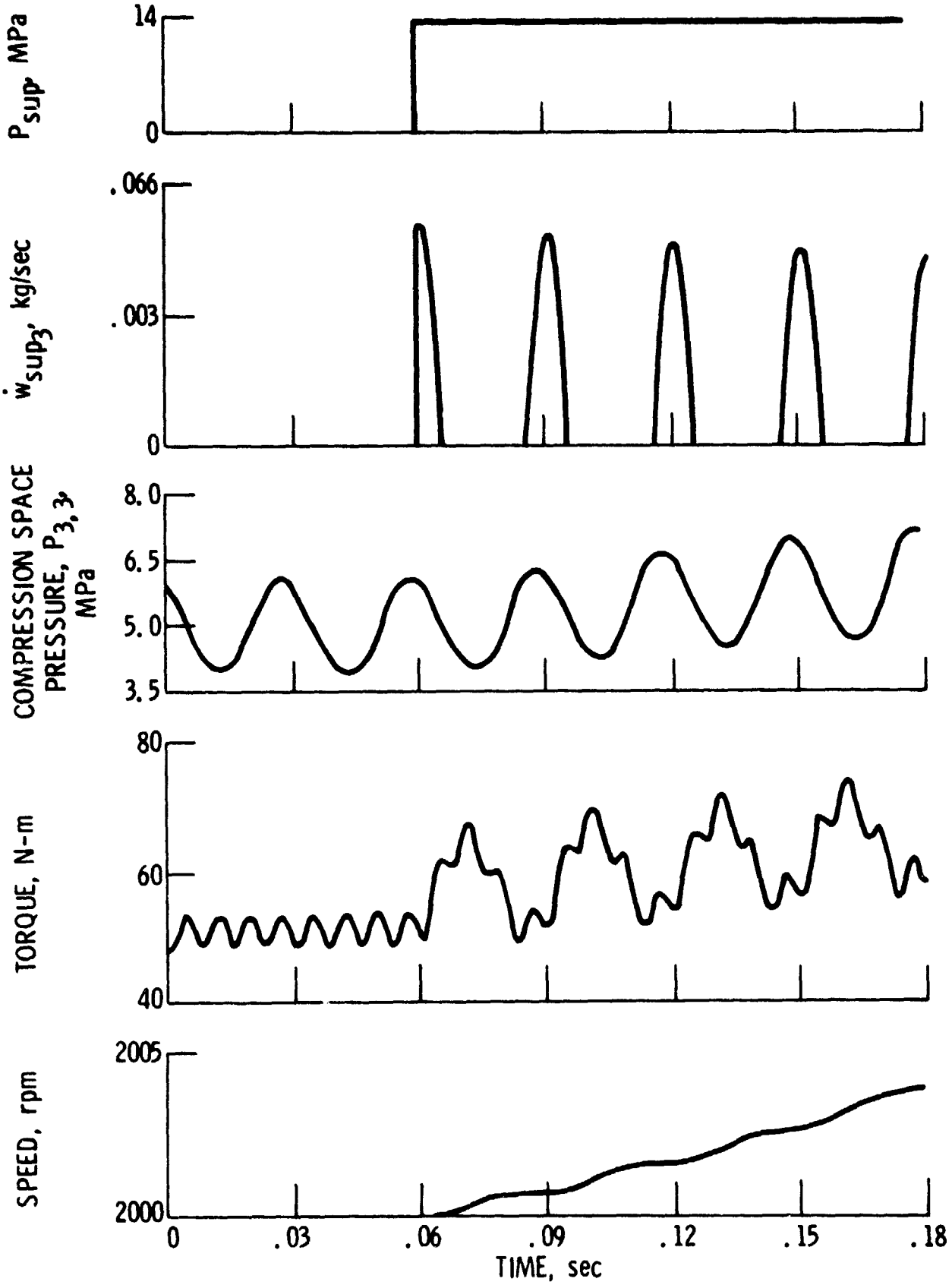

Figure 7. - Working fluid supply transient P_{sup} = 13.8 MPa at T = 0.06 sec.

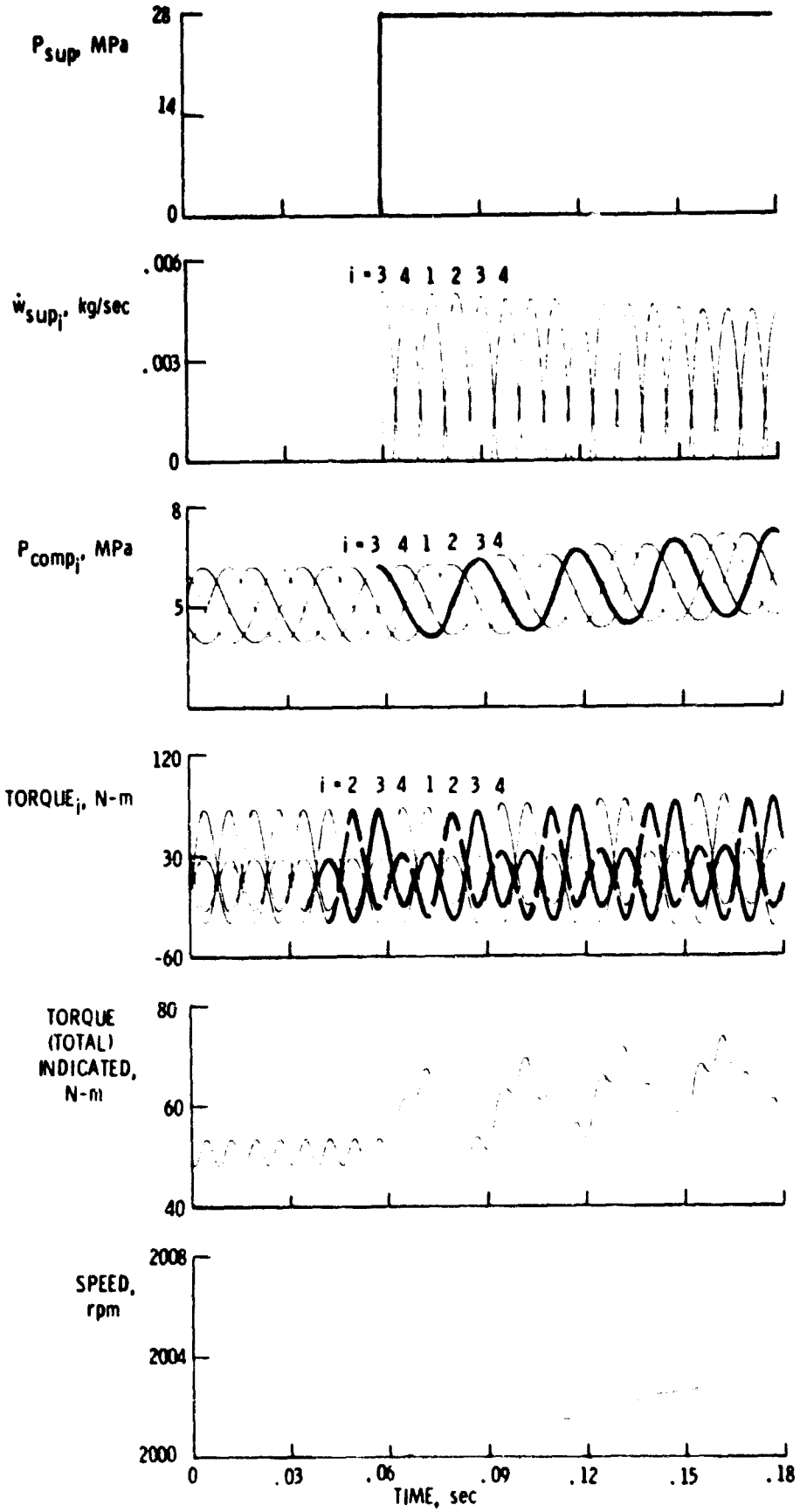

Figure 8. - Detailed working fluid supply transient, no rod leakage, P_{sup} = 13.8 MPa at t = 0.06 sec.

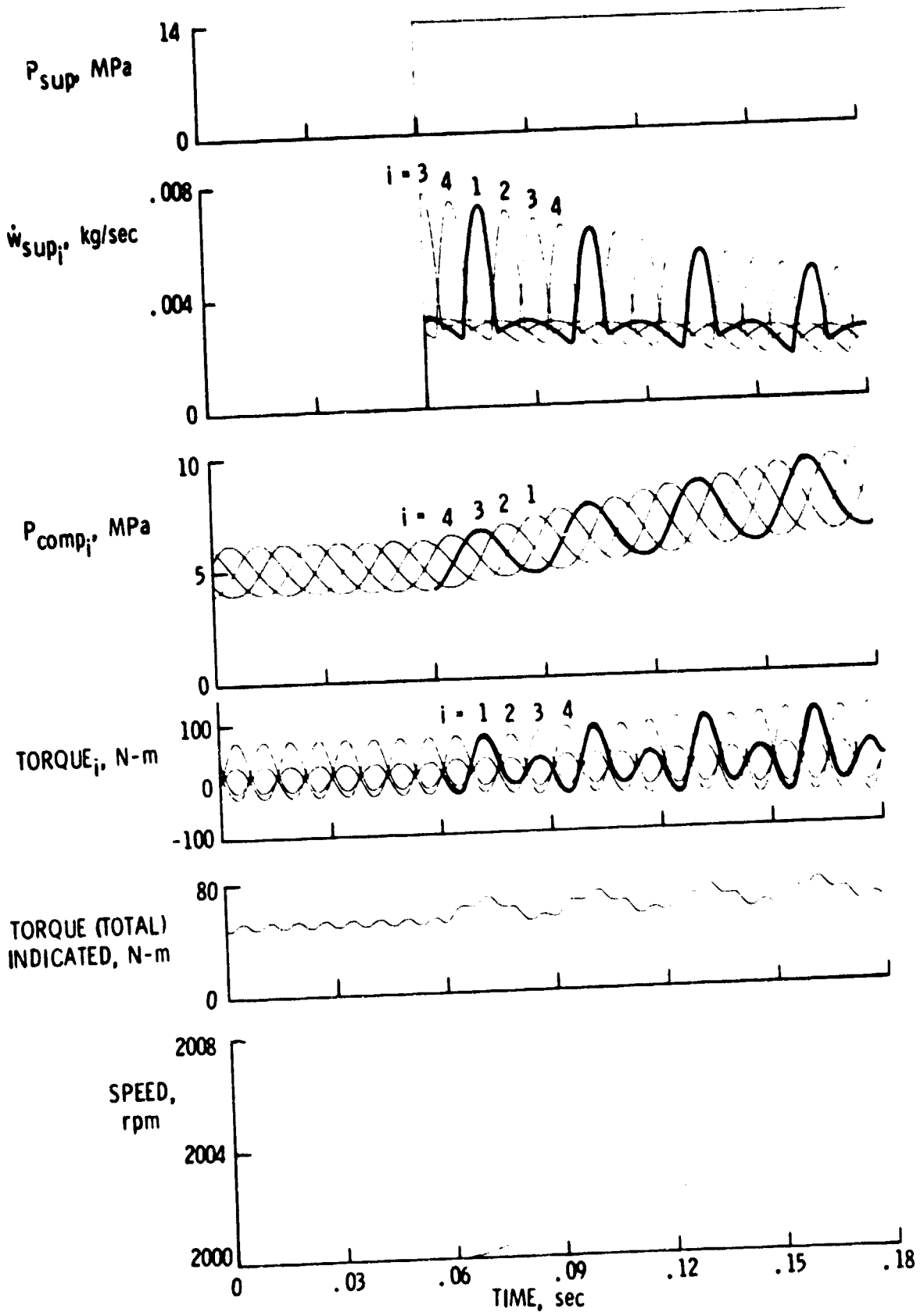

Figure 9. - Working fluid supply transient with uniform piston rod leakage. $A_{r\ell_i} = 0.5\, A_{imax}$, $P_{sup} = 13.8$ MPa at $t = 0.06$ sec.

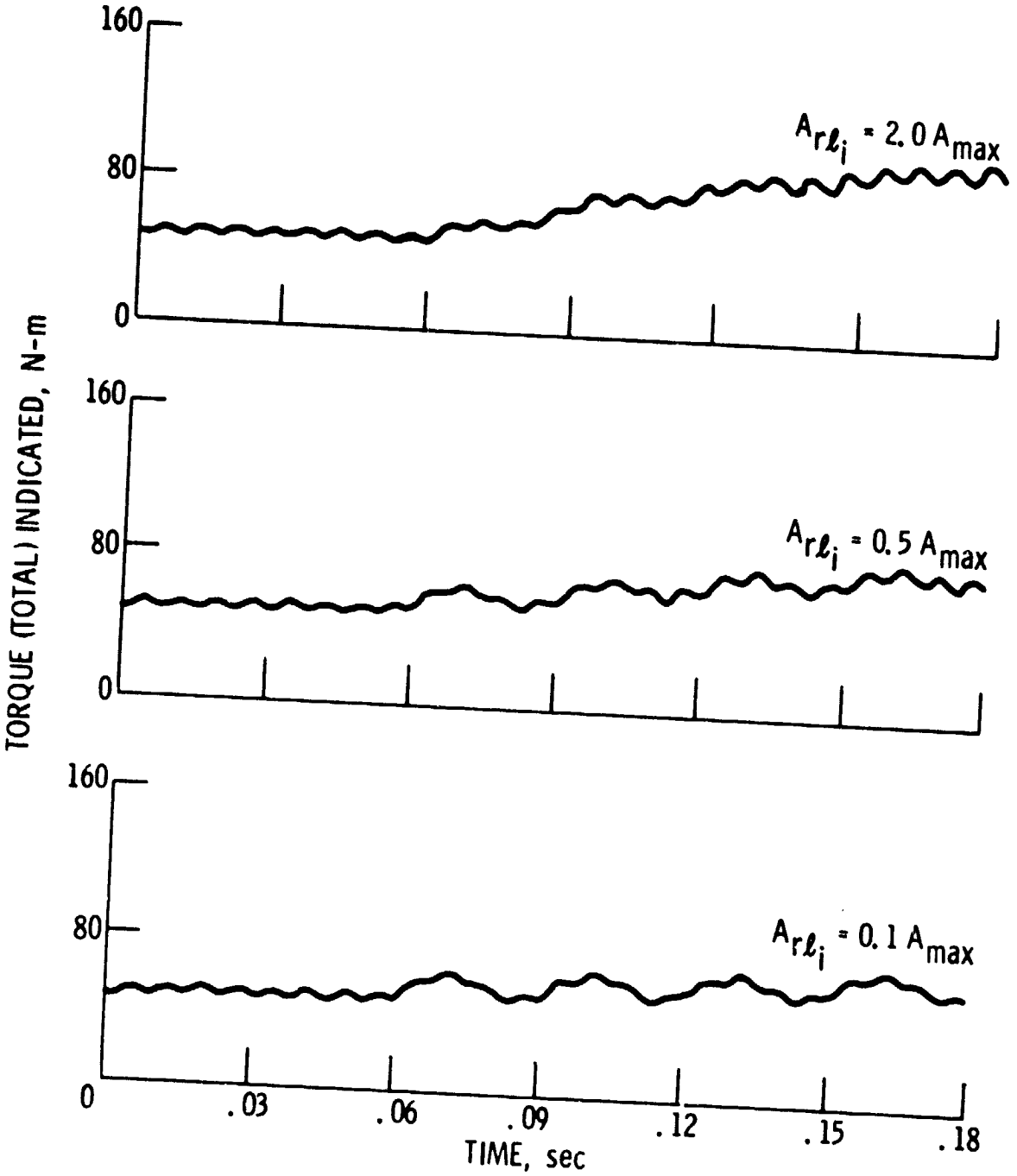

Figure 10. - Effect of various piston rod leakage rates on total indicated torque response. Uniform leakage rate all piston rods. $P_{sup} = 13.8$ MPa at $t = 0.06$ sec.

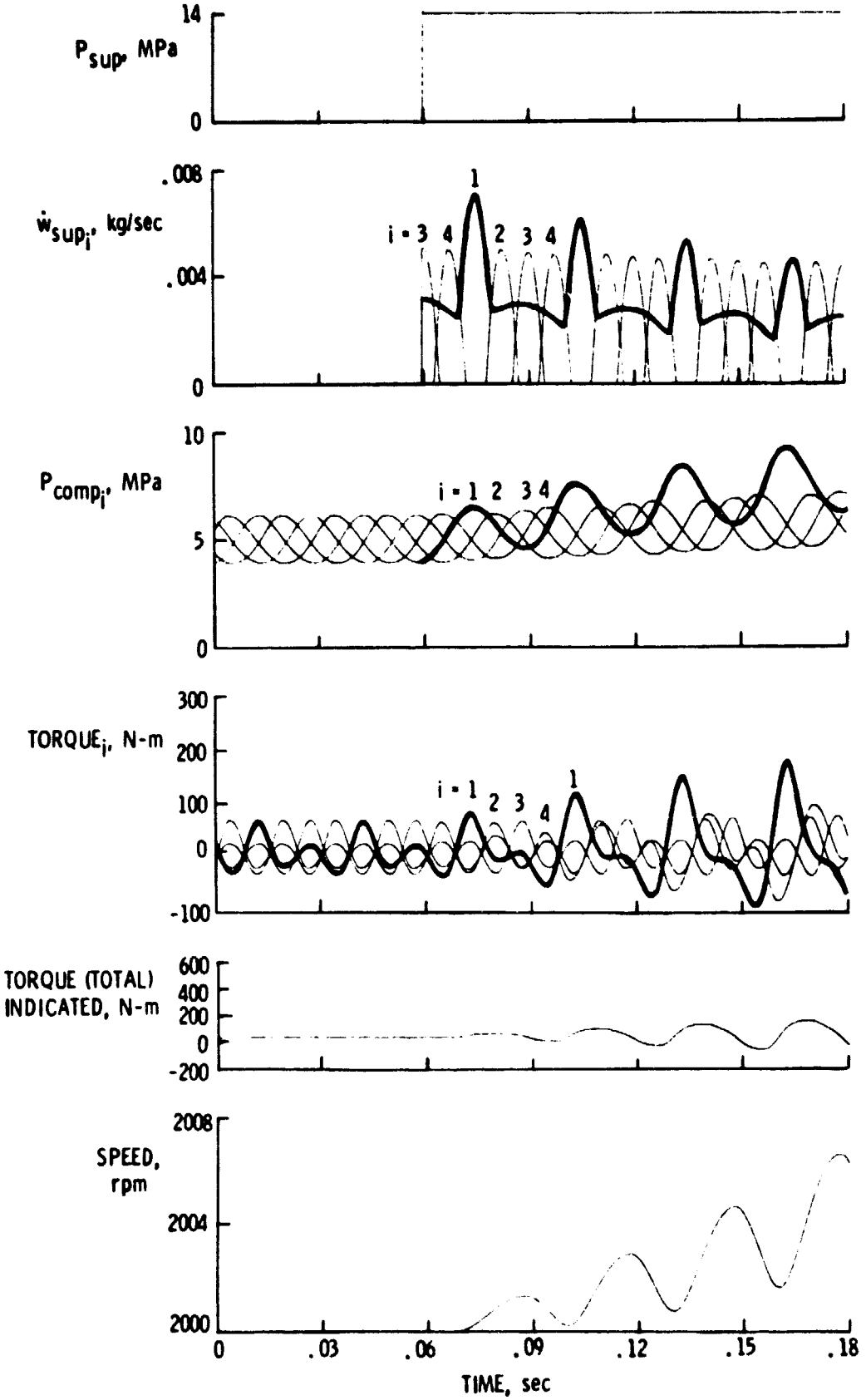

Figure 11. - Effect of single piston rod leak. P_{sup} = 13.8 MPa at t = 0.06 sec; $A_{r\ell_1} = 0.5\, A_{1max}$.

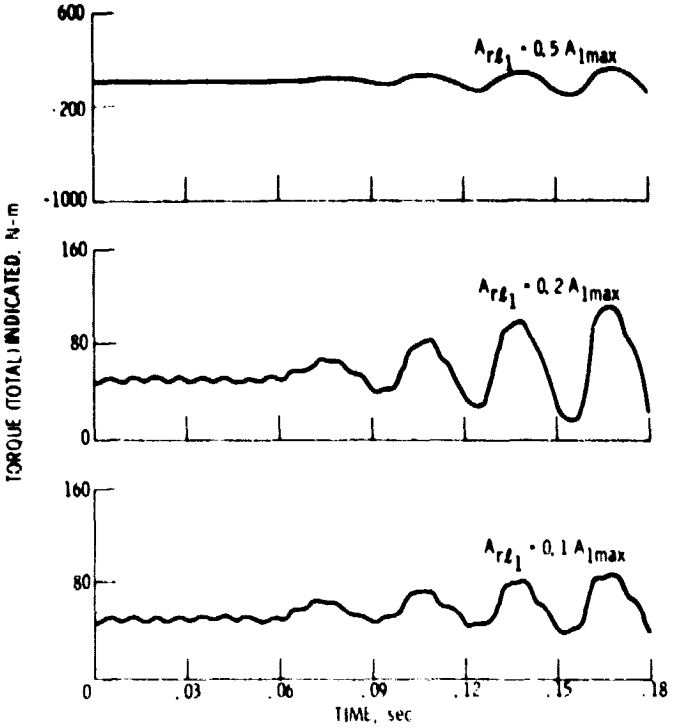

Figure 12. - Effect of piston rod leakage rate on total indicated torque response. Single piston rod leak. $P_{sup} = 13.8$ MPa at $t = 0.0$b sec.

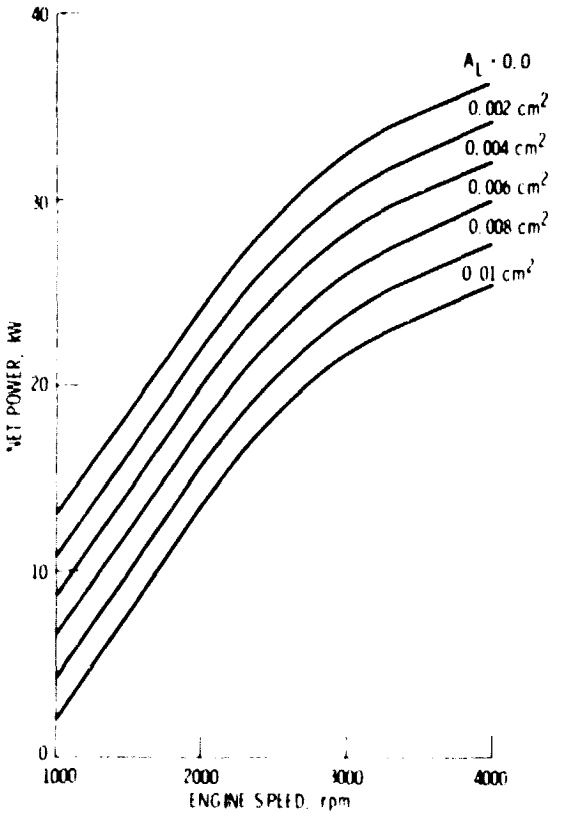

Figure 13. - Net power versus speed for various piston ring leakage areas, $\bar{P} = 15$ MPa.

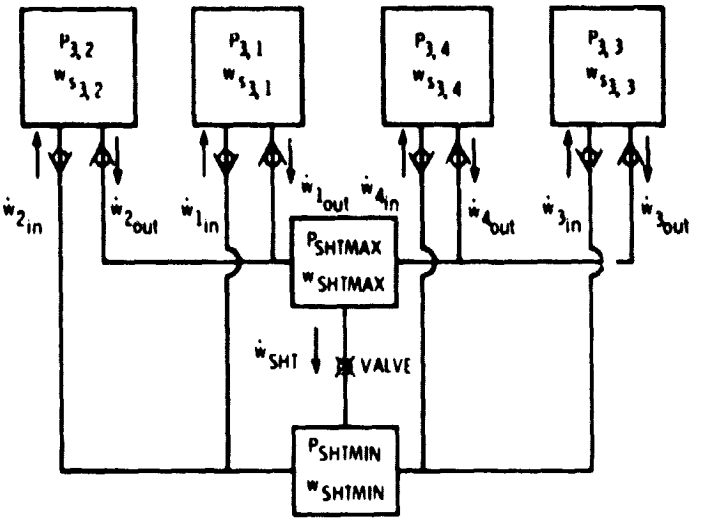

Figure 14. - Schematic of short circuit system.

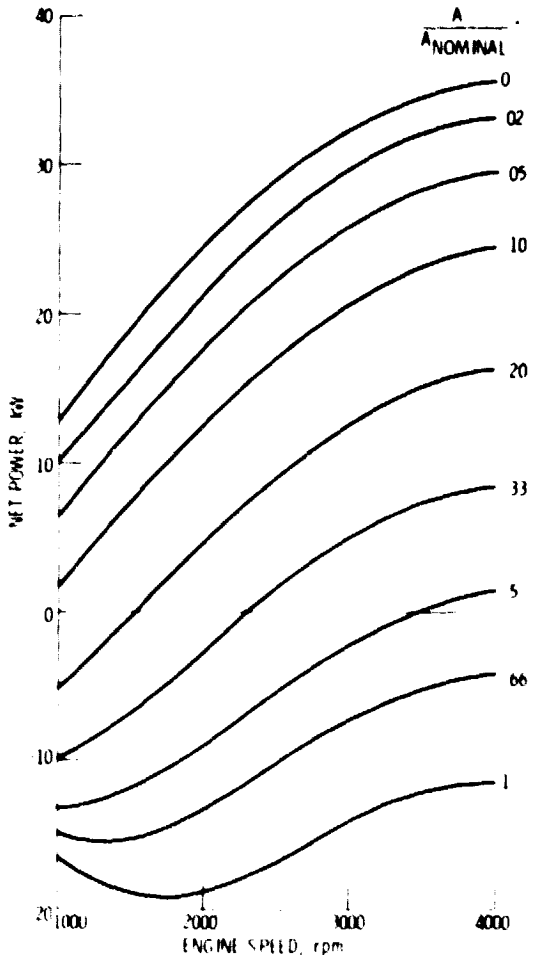

Figure 15. Net power for various short circuit valve areas. $\bar{P}$ = 15 MPa.

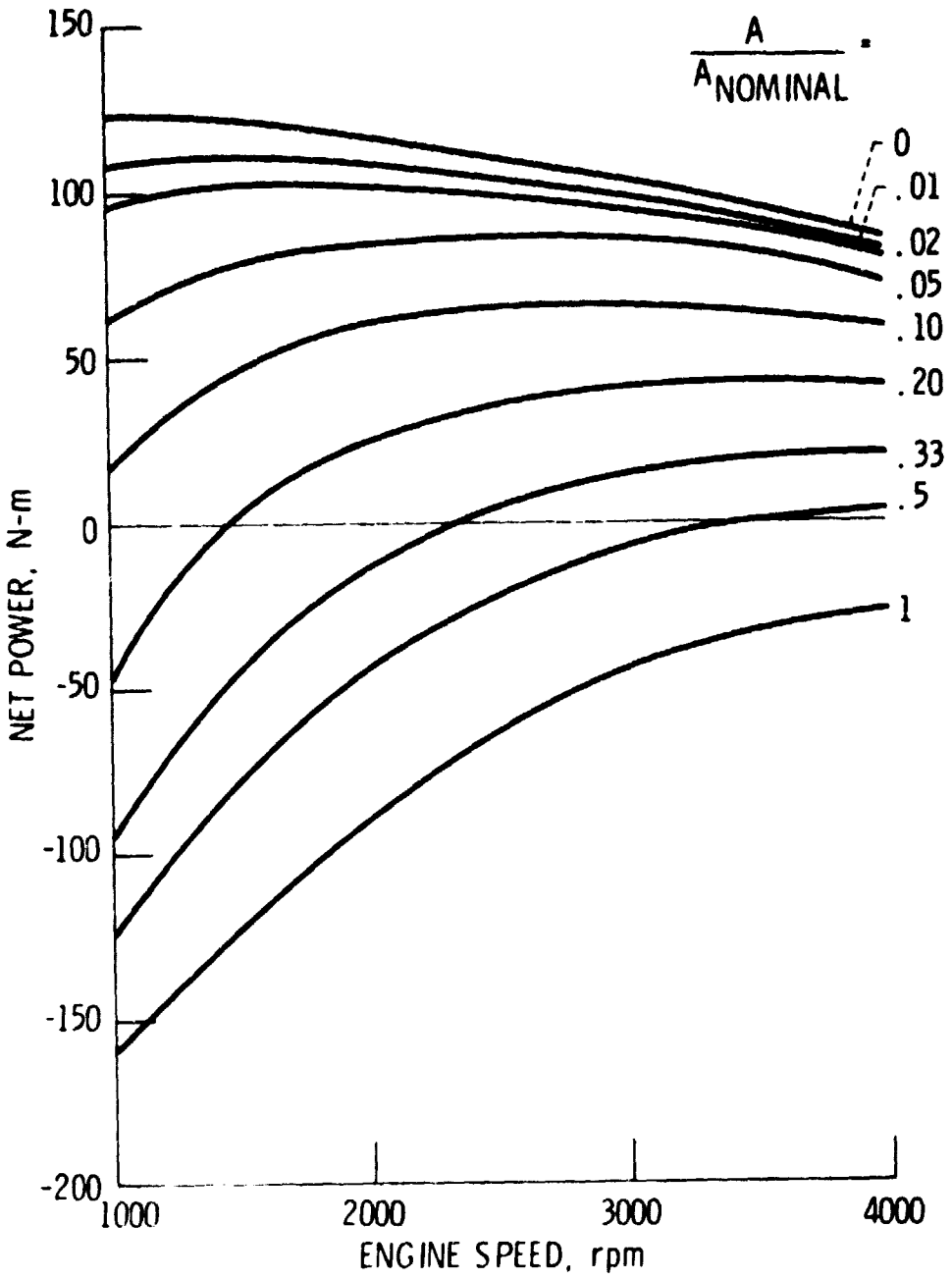

Figure 16. - Net torque for various short circuit valve areas. $\bar{P}$ = 15 MPa.